Supporting Information

Memarzadeh et al. 10.1073/pnas.1105243108

SI Materials and Methods

Experimental Animals. Animals were maintained on 12-h light and dark cycles according to UCLA DLAM protocol. Timed mating was set up between heterozygous Tfm female and WT male mice. Embryonic day 16–17 mice were harvested, and mice were genotyped for the presence of the Y chromosome and Tfm mutation as described (1) (Table S1). AR^{flox}/Y transgenic mice were bred and genotyped according to established protocols (2).

Plasmids. To make the FU-CreRFP lentiviral vector, cDNAs of RFP and Cre recombinase were fused through PCR-based method. A 22-aa linker was inserted between RFP and Cre (peptide: GESSGSISSLSTVNAPKKKRKV coded by the nucleotide sequence: GGAGAGAGTTCTGGCAGCATCTCCTCCCTGAG CACTGTTAACGCACCCAAGAAGAAGAGGAAGGTG). The RFP and Cre fusion cDNA were cloned into FUGW (3) at the XbaI site. To construct the FU-Cre-CRW vector, the cDNA for Cre was cloned into the EcoRI site of the FU-CRW vector. The FU-Cre-CRW vector was used to facilitate sorting of infected cells, because the RFP driven by an independent promoter in this vector is bright in signal.

To construct the shRNA-mAR vector, the murine AR-specific short hairpin RNAs (shRNA) (4) with a U6 promoter were cloned into the BamHI-EcoRI site the lentivector FUCRW. The ORF for the human AR gene with flag tag was cloned at the XbaI site under the human ubiquitin promoter to yield the shRNA-mAR+hAR vector.

To construct the FUCRW-mAKT-IRES-Cre lentiviral vector, ERG cDNA fragment in FUCRW-AKT-IRES-ERG (5) was replaced by Cre.

Immunohistochemistry. The primary antibodies used were as follows: anti-AR (sc-816), anti-AR (sc-815) and anti-p63 (sc-8431) were from Santa Cruz Biotechnology, anti-CK5 (PRB-160P) and anti-CK8 (MMS-162P) from Covance, anti-AKT (9272), anti-phosphoAKT (3787), and anti-cyclin D1 (2978) were from Cell Signaling Technologies, anti-ER α (clone ID5, M7047) was from Dako, and anti-pancytokeratin (C1801, Sigma). Additional reagents were biotinylated anti-rabbit (111-065-003) and SA-HRP (016-010-084) from Jackson Immunoresearch, biotinylated anti-mouse M.O.M. kit (BMK-2202) from Vector Laboratories, and DAB chromogen (HK130-5K) from Biogenex. TUNEL assay was performed by using the in situ cell death detection kit from Roche (11-684-817-910). Counterstaining for fluorescent imaging was done with DAPI (Vector Laboratories).

Western Blots. A RIPA buffer was used for lysing cells as described (6). Antibodies used for Western blot were as follows: anti-AKT (9272), anti-phosphoAKT (3787), anti-AR (sc-816), anti-Cre (Novagen 69050), and anti-ERK2 (Santa Cruz sc-154).

Quantitative PCR. RNA was extracted by using Qiagen RNeasy Mini kit according to manufacturer instructions. Reverse transcription was performed with a SuperScript III first-strand synthesis system (Invitrogen). Q-PCR was performed by using iQ SYBR Green Supermix for Real-Time PCR (Bio-Rad) on a Bio-Rad iCycler and iQ5 2.0 Standard Edition Optical System Software with primers specific for FGF10 (6). Data were analyzed by using the Pfaffl method.

Laser Capture Microdissection. DNA was extracted from LCM tissue by using the QIAamp DNA FFPE kit according to manufacturer instructions. Cre DNA was detected by using two sequential rounds of PCR amplification (30 cycles each) using primers as listed (Fig. S6). Putative cre bands identified on TAE-agarose gels were excised, extracted, and sequenced.

Quantification of Prostate Tubules in the Regenerated Grafts. Regenerated grafts were paraffin embedded and sectioned. Hematoxylin and eosin (H&E) staining was performed on every five sequential sections. Sections were examined by a pathologist who was blinded to the treatment. In the FGF10-tumor grafts, the area of tissue involved by the tumor was recorded as a percentage of tumors in the whole regenerated tissue on each slide. Results were averaged from five slides spanning the entire graft over 30 sequential tissue sections. Error bars represent SD. Statistical significance was determined by using two-tailed *t* test.

1. Gao J, Isaacs JT (1998) Development of an androgen receptor-null model for identifying the initiation site for androgen stimulation of proliferation and suppression of programmed (apoptotic) death of PC-82 human prostate cancer cells. *Cancer Res* 58:3299–3306.
2. De Gendt K, et al. (2004) A Sertoli cell-selective knockout of the androgen receptor causes spermatogenic arrest in meiosis. *Proc Natl Acad Sci USA* 101:1327–1332.
3. Lois C, Hong EJ, Pease S, Brown EJ, Baltimore D (2002) Germline transmission and tissue-specific expression of transgenes delivered by lentiviral vectors. *Science* 295:868–872.
4. Jiao J, et al. (2007) Murine cell lines derived from Pten null prostate cancer show the critical role of PTEN in hormone refractory prostate cancer development. *Cancer Res* 67:6083–6091.
5. Zong Y, et al. (2009) ETS family transcription factors collaborate with alternative signaling pathways to induce carcinoma from adult murine prostate cells. *Proc Natl Acad Sci USA* 106:12465–12470.
6. Memarzadeh S, et al. (2007) Enhanced paracrine FGF10 expression promotes formation of multifocal prostate adenocarcinoma and an increase in epithelial androgen receptor. *Cancer Cell* 12:572–585.

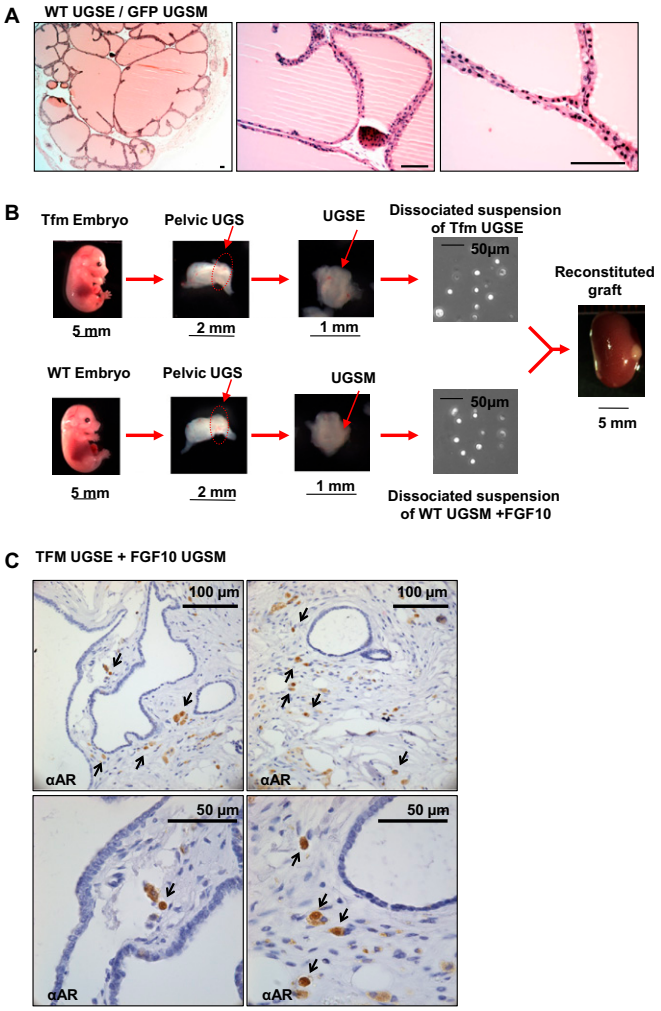

Fig. S1. Experimental scheme for regeneration of dissociated UGSE. (*A*) Dissociated populations of embryonic UGSE combined with UGSM could regenerate into prostate-like glands. The 10^5 WT UGSE cells were combined with 10^5 WT UGSM and placed in the in vivo prostate regeneration system for 8 wk. Prostate-like glandular structures containing secretions were formed similar to results obtained in regenerations by using adult prostate epithelia. (Scale bars: 100 µm.) (*B*) Microdissected UGSE was harvested from WT or Tfm (genotyped) E16–17 male embryos. UGSE was dissociated with collagenase digestion and recombined with FGF10-expressing UGSM. Cellular combinations were regenerated under the mouse kidney capsule to assess response of Tfm vs. WT UGSE to paracrine FGF10. (*C*) Expression of nuclear AR is detected in grafts regenerated from recombination of Tfm UGSE and FGF10-expressing UGSM.

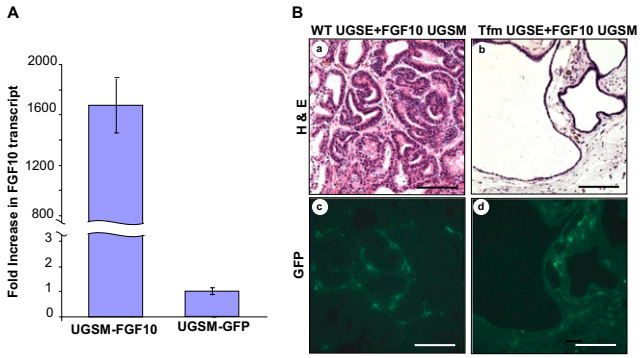

Fig. S2. Confirmation of FGF10 overexpression in infected UGSM cells. (*A*) UGSM were infected with MSCV-FGF10-IRES -GFP or MSCV-IRES-GFP retroviruses. Messenger RNA levels of FGF10 was measured and compared in the FGF10 vs. GFP-expressing UGSM cells by using quantitative PCR. One example of such analysis showing a dramatic increase in FGF10 message is shown. Error bars represent one SD. (*B*) GFP marks the site of stromal FGF10 expression (*c, d*) in regenerated grafts (*a, c*). GFP is expressed faithfully by an IRES in the MSCV retroviral vector used for the overexpression of FGF10 and can be visualized by using fluorescent microscopy. (Scale bars: 100 µm.)

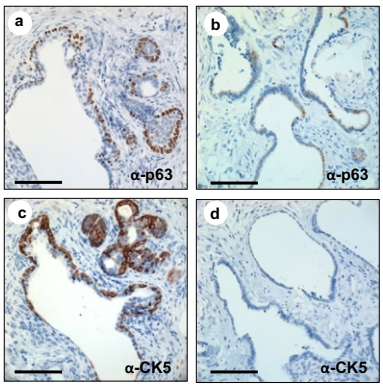

Fig. S3. Pattern of expression for basal cells in Tfm-regenerated grafts with add back of AR. After add back of AR, there was an expansion of cells expressing basal markers p63 (*A*) and CK5 (*C*) in hyperplastic regions. Adjacent nonhyperplastic, AR null tubules in the same graft expressed p63 (*B*) but not CK5 (*D*). (Scale bars: 100 μm.)

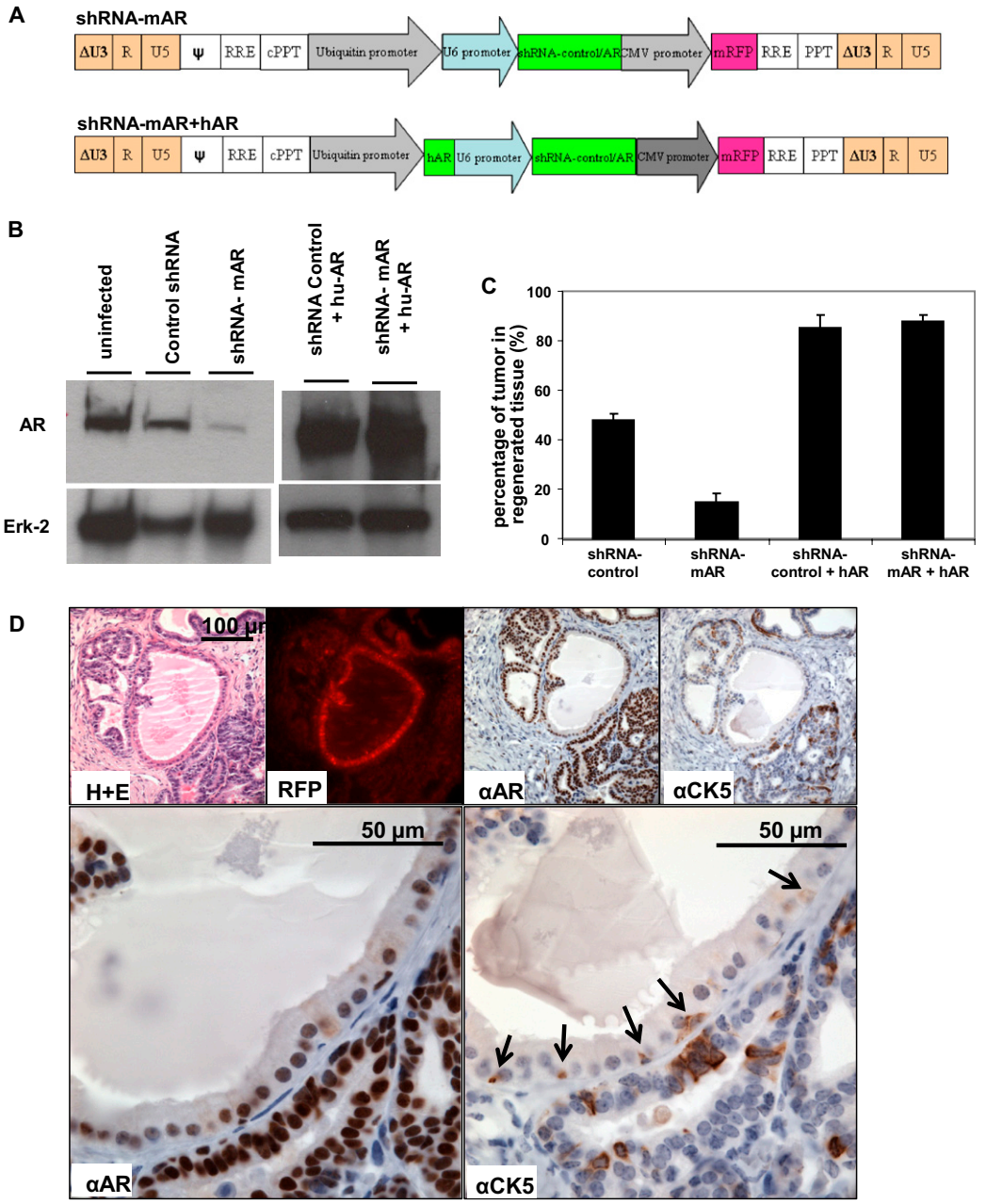

Fig. S4. Silencing and add back of AR in adult prostate epithelium was achieved by using lentiviral delivery vectors. (*A*) The knockdown of AR was achieved by using shRNA-mAR lentiviral expression vector. Knockdown of mouse AR and overexpression of human AR was achieved by using the shRNA-mAR+hAR lentiviral construct. The human AR construct was flag tagged. (*B*) Western blot analysis confirming function of both lentiviral constructs. Tramp C2 cells were infected with shRNA-control, shRNA-mAR, shRNA-control+hu-AR, or shRNA-mAR+hu-AR lentivirus. The infected cells were sorted by FACS based on expression of marker RFP (color marker expressed in all vectors). Infected cells were lysed and analyzed for expression of AR with Western blot. (*C*) Percentage of tumor in the regenerated tissue was quantified and compared among all grafts. The percentage of tumor area in the regenerated tissue was significantly decreased with loss of epithelial AR (shRNA-control vs. shRNA-mAR; $P < 0.0001$). Add back of hAR could restore response to FGF10 demonstrated by increased areas of hyperplastic tubules (shRNA-mAR vs. shRNA-mAR+hAR, $P < 0.0001$). (*D*) Expression of shRNA-mAR resulted in formation of normal appearing prostate tubules with relatively lower expression of AR compared with adjacent hyperplastic glands. RFP marks the site of expression for shRNA-mAR in these grafts. These normal-appearing RFP-positive tubules contain basal cells expressing the marker CK5.

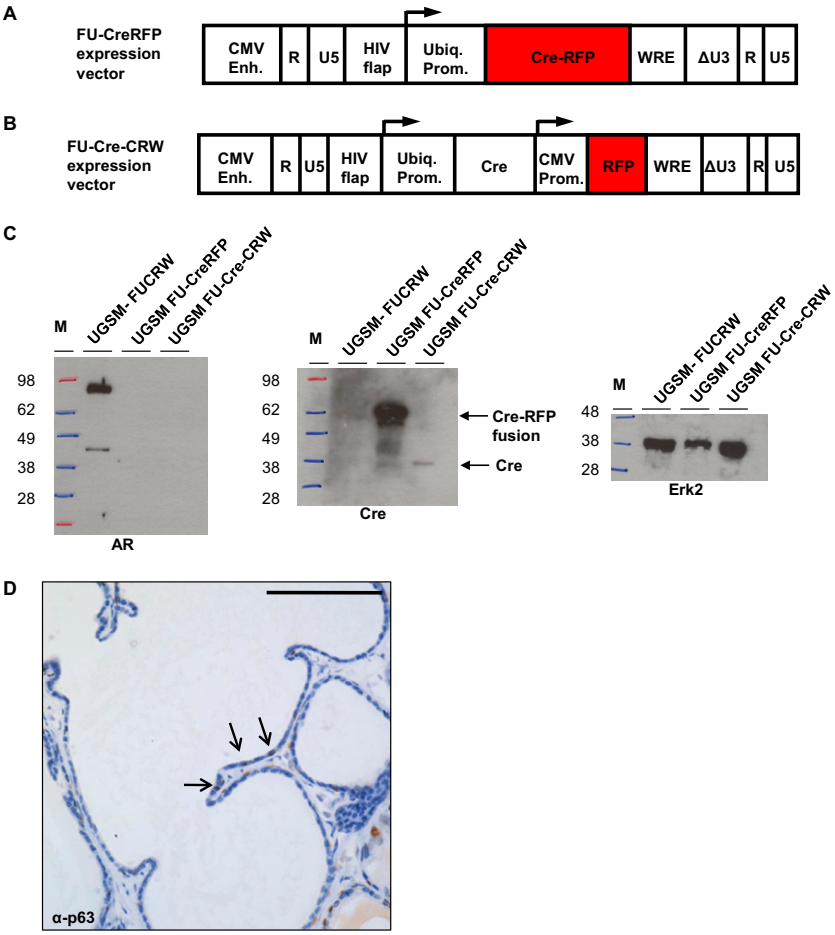

Fig. S5. Cre recombinase was expressed in AR ^{flox}/Y adult prostate epithelium by using lentiviral expression constructs. (*A*) The lentivirus FU-CreRFP was used to express an RFP and Cre fusion cDNA. Because this is a fusion gene, the RFP signal was dim. (*B*) To improve the detection of RFP signal in the Cre-expressing lentiviral vector, Cre and RFP were driven by independent promoters in the same lentiviral vector, FU-Cre-CRW, resulting in a brighter RFP signal. (*C*) AR-loxP UGSM cells, harvested from E16–17 AR-loxP embryos, were infected with control (FUCRW), FUCRW-CreRFP, or FU-Cre-CRW viruses. Western blot on protein lysates confirmed presence of Cre and absence of AR in the Cre-infected UGSM. Erk2 was used as a loading control. (*D*) Only a few p63-positive cells were detected in regenerated atrophic AR-null prostate glands. (Scale bars: 50 μm.)

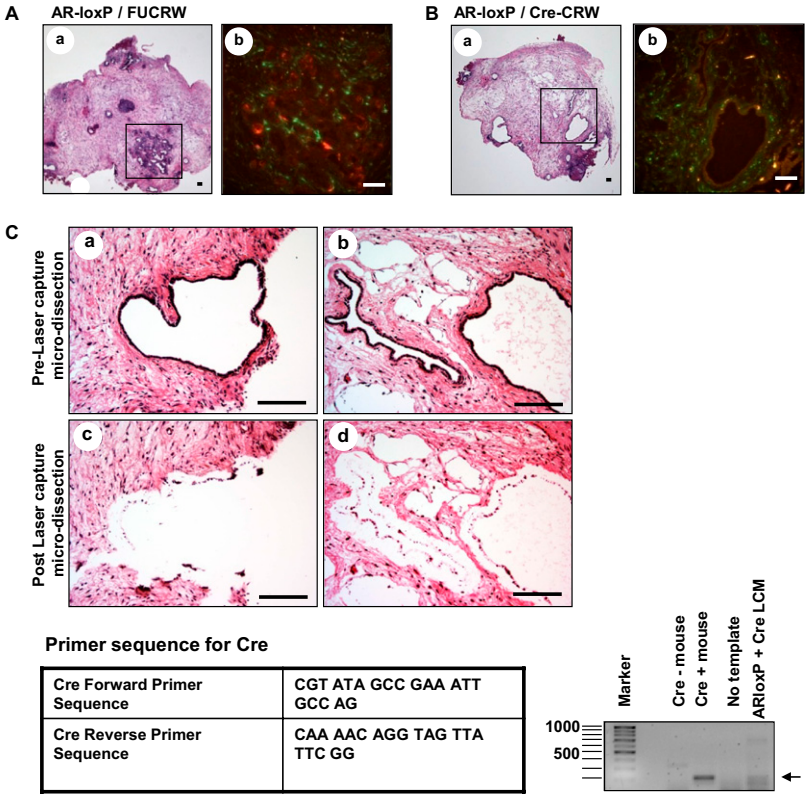

Fig. S6. Expression of Cre in adult prostate epithelia of AR ^{flox}/Y resulted in a general diminution in regeneration and development of atrophic tubules despite paracrine FGF10 signals. (*A*) Hyperplastic glands formed in control epithelia in response to stromal FGF10 signals (*a*). RFP was expressed in the epithelium marking expression of FUCRW control vector (*b*). GFP expression in the stroma marked the expression site for FGF10 (*b*). (*B*) Loss of AR resulted in regeneration of atrophic tubules (*a*). Regenerated atrophic tubules expressed RFP in the epithelium (marking the expression site for Cre) and stromal GFP as an indirect marker for expression of FGF10 (*b*). (*C*) Atrophic prostate glands regenerated in FU-Cre-CRW/FGF10 grafts were isolated by laser capture microdissection. Examples of representative sections are shown pre- and postmicrodissection (*a* vs. *c* and *b* vs. *d*). (Scale bars: 100 μm.) DNA was extracted and amplified by using primers for Cre (listed in table). As a positive control, genomic DNA from a Cre-expressing transgenic mouse was used. The PCR-amplified product from atrophic prostate tubules, visualized on gel, was isolated and sequenced confirming expression of Cre in the atrophic regenerated prostate glands.

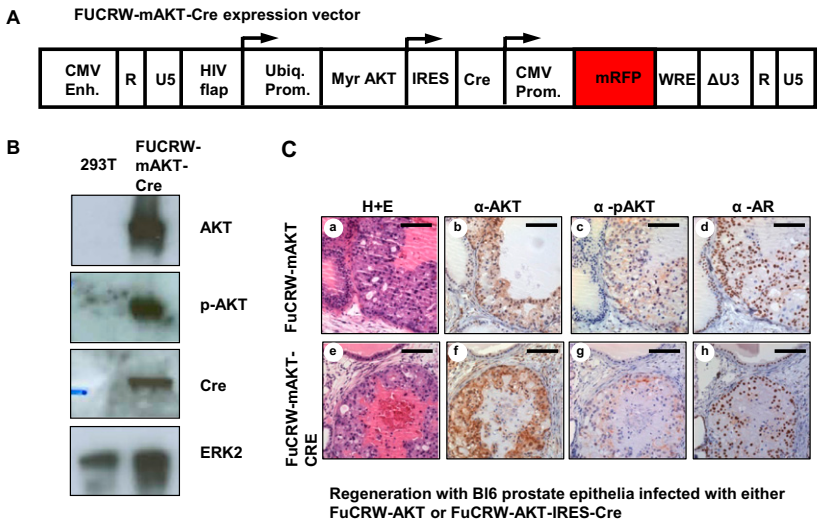

Fig. S7. Expression of myristoylated AKT and Cre was achieved in adult prostate epithelium by using one lentiviral delivery vector. (*A*) A single lentiviral expression vector was used for expression of myristoylated AKT and Cre in primary adult prostate epithelium. This construct also expressed RFP marking the site of expression for this viral vector. (*B*) Western blot analysis confirmed expression of myristoylated AKT and Cre in this lentiviral construct. 293T cells were infected with this lentivirus and expression of Cre and phosphorylated AKT was confirmed by Western blot. (*C*) Expression of FuCRW-mAKT-Cre vector resulted in the formation of PIN in naïve adult prostate epithelium. Similar to the FuCRW-mAKT vector (*a*–*d*), expression of this newly designed lentiviral construct FuCRW-mAKT-Cre could lead to the development of PIN lesions in primary WT adult prostate epithelium (*e*–*h*).

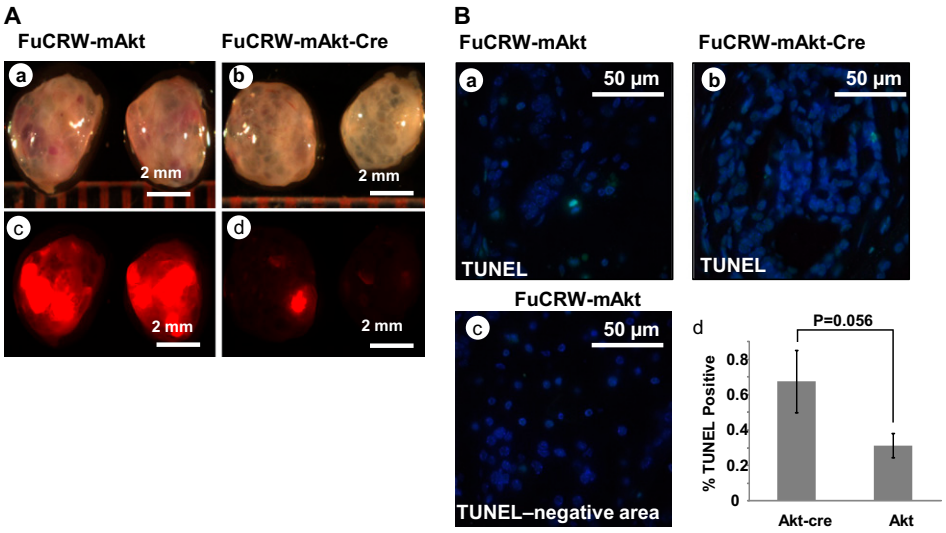

Fig. S8. Comparison of FUCRW-mAKT and FUCRW-mAKT-Cre regenerated tissue. (*A*) Transilluminating and fluorescent images of grafts regenerated from AR-loxp prostate epithelia infected with FUCRW-mAKT (*a*, *c*) or FUCRW-mAKT-Cre (*b*,*d*). (*B*) A significant difference in the number of apoptotic cells was not detected between AR-null and AR-WT regenerated tubules expressing activated AKT (*d*). TUNEL assay was performed on AR null (*b*) or AR-WT (*a*, *c*) grafts for detection of apoptotic cells. Results are expressed as the average % positive ±1 SD. (Scale bars: 50 µm.)

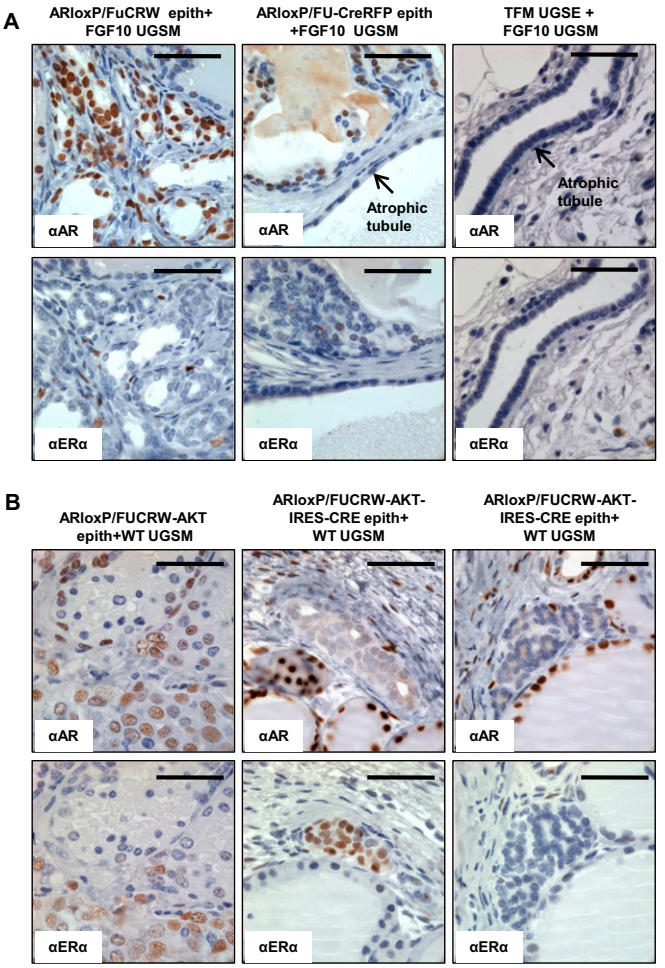

Fig. S9. Expression of ER α in FGF10 and AKT-regenerated grafts. (*A*) Expression of ER α was examined in ARloxP/FUCRW epith+FGF10 UGSM, ARloxP/FU-CreRFP epith+FGF10 UGSM, and TFM UGSE+FGF10 UGSM-regenerated grafts. Predominance of these regenerated epithelia (AR WT and AR-null) had low or undetectable levels of ER α expression. (*B*) ER α expression was also examined in ARloxP/FUCRW-AKT+WT UGSM and ARloxP/FUCRW-AKT-IRES-CRE+WT UGSM-regenerated grafts. Variable levels of ER α expression were detected in both AR-WT and AR-null AKT-initiated hyperplastic regions. Some hyperplastic areas expressed high levels of nuclear ER α, whereas other areas had low or undetectable levels of ER α expression.

Table S1. Protocol for genotyping Tfm embryos and adult male mice

Gene	Primer pair
Primers in the AR gene used to identify Tfm mutation	5′-CCCGTCCTCTCTGTCTCTGT-3′
	5′-TGCCGTAGTCCAATGGGTTC-3′
SRY primers used to determine the sex	5′-CTGCAGTTGCCTCAACAAAA-3′
	5′-AAACTGCTGCTTCTGCTGGT-3′

To identify Tfm male embryos and adult mice a 166-bp product of the AR gene was amplified from genomic DNA (1). This product was cut with MWo-1 enzyme (1). The Tfm PCR product remained uncut, whereas the WT band was cut into 110- and 56-bp products (1). Sex of the embryos was confirmed by PCR amplification of SRY gene using the primer set in Table S1. Presence of an SRY band indicated a male progeny.